AFRL-AFOSR-UK-TR-2020-0022

Modeling of Chromophores under Static Electric Fields for Preparation of Ordered Bulk Glass Materials with Superior Optical Power Limiting Properties

Patrick Norman
KUNGLIGA TEKNISKA HOGSKOLAN
VALHALLAVAGEN 79
STOCKHOLM, 10044
SE

07/02/2020
Final Report

Air Force Research Laboratory
Air Force Office of Scientific Research
European Office of Aerospace Research and Development
Unit 4515 Box 14, APO AE 09421

REPORT DOCUMENTATION PAGE

Form Approved
OMB No. 0704-0188

1. REPORT DATE *(DD-MM-YYYY)*	2. REPORT TYPE	3. DATES COVERED *(From - To)*
02-07-2020	Final	15 Jan 2017 to 14 Jan 2020

4. TITLE AND SUBTITLE
Modeling of Chromophores under Static Electric Fields for Preparation of Ordered Bulk Glass Materials with Superior Optical Power Limiting Properties

5a. CONTRACT NUMBER

5b. GRANT NUMBER
FA9550-17-1-0061

5c. PROGRAM ELEMENT NUMBER
61102F

6. AUTHOR(S)
Patrick Norman

5d. PROJECT NUMBER

5e. TASK NUMBER

5f. WORK UNIT NUMBER

7. PERFORMING ORGANIZATION NAME(S) AND ADDRESS(ES)
KUNGLIGA TEKNISKA HOGSKOLAN
VALHALLAVAGEN 79
STOCKHOLM, 10044 SE

8. PERFORMING ORGANIZATION REPORT NUMBER

9. SPONSORING/MONITORING AGENCY NAME(S) AND ADDRESS(ES)
EOARD
Unit 4515
APO AE 09421-4515

10. SPONSOR/MONITOR'S ACRONYM(S)
AFRL/AFOSR IOE

11. SPONSOR/MONITOR'S REPORT NUMBER(S)
AFRL-AFOSR-UK-TR-2020-0022

12. DISTRIBUTION/AVAILABILITY STATEMENT
A DISTRIBUTION UNLIMITED: PB Public Release

13. SUPPLEMENTARY NOTES

14. ABSTRACT
Influence of the viscosity of the solvent on the molecular motions, orientation of the molecule in the electric fields, the evaporation process, and concentration effects were successfully studied and described by molecular dynamic (MD) simulations. Our calculations have shown that the presence/absence of electric fields and the length of solvent molecules (degree of polymerization, viscosity) influence the motion of the molecules of interest. Moreover, by specific and targeted substitutions of donor and acceptor groups, we were able to design novel molecules suitable for optical power limiting (OPL) purposes. The successful results of our theoretical work have stimulated our experimental partners at the Swedish Defence Research Agency (Dr. Cesar Lopes) and University of Lyon (Prof. Stephane Parola) to develop synthetic protocols and equipment to produce ordered bulk glass materials in the laboratory.

15. SUBJECT TERMS
EOARD, Optical power limiting, Nonlinear optics, Bulk glass, Chromophores, Polarization

16. SECURITY CLASSIFICATION OF:			17. LIMITATION OF ABSTRACT	18. NUMBER OF PAGES	19a. NAME OF RESPONSIBLE PERSON
a. REPORT	b. ABSTRACT	c. THIS PAGE			FOLEY, JASON
Unclassified	Unclassified	Unclassified	SAR		19b. TELEPHONE NUMBER *(Include area code)* 011-44-1895-616036

Standard Form 298 (Rev. 8/98)
Prescribed by ANSI Std. Z39.18

FINAL REPORT July 1, 2020

Grant Number: FA9550-17-1-0061

Title: Modelling of Chromophores under Static Electric Fields for Preparation of Ordered Bulk Glass Materials with Superior Optical Power Limiting Properties

PI Name: Prof. Patrick Norman (KTH)

Co-PIs: Assoc. Prof. Mathieu Linares (KTH) together with experimentalists Dr. Cesar Lopes (FOI) & Dr. Stephane Parola (CNRS, Lyon)

Researchers: Dr. Michal Biler (KTH)

Period of Performance: 15 Jan 2018 – 14 Jan 2020

Keywords: optical power limiting, platinum(II) acetylide, electric dipole orientation, electric field, glass material, molecular dynamics

Contact:

Patrick Norman, Professor
Department of Theoretical Chemistry and Biology
KTH Royal Institute of Technology
SE-106 91 Stockholm, Sweden
Homepage: https://www.kth.se/tcb

e-mail: panor@kth.se
phone : +46 8 790 96 31
mobile: +46 73 765 2253

Table of Content

List of Figures

V/nm) from orientation on the left side (the $NO_2 \rightarrow NH_2$ vector being antiparallel to the electric field propagation) to the orientation on the right side (the $NO_2 \rightarrow NH_2$ vector being parallel to the electric field propagation).

Figure 8 - Population of the angles for DEANST in the presence of electric field (EE = 0.43 V/nm).

Figure 9 - Population of PN1 and its development over time in the presence of electric field (EE = 0.43 V/nm).

Figure 10 – Evolution of evaporation process for DEANST. MTE-1 in red, THF in blue.

Figure 11 – Density (left) and volume (right) evolvements during the evaporation effect. Black curve corresponds to the box with THF and MTE-1, the red curve to THF and MTE-3, and the blue curve to THF and MTE-5.

Figure 12 – Proposed structures of molecules for OPL. Red vector shows the vector taken to evaluate the orientation angle.

Figure 13 – Population of orientation angles for molecule **1** and its development over time.

Supplementary information

Figure S1 – Orientation and omega angles' population of PFF in the absence of electric field.

Figure S2 – Orientation and omega angles' population of PFF in the presence of electric field (EE = 0.43 V/nm). Detailed time development for PFF in THF and MTE-7 shown in Fig. S3.

Figure S3 – PFF in THF and MTE-7 and its development over a period of 40 ns.

Figure S4 – Omega angles' population for PN1 with the electric field (EE = 0.43 V/nm).

Figure S5 – Population of PE2 and its development over time in electric field (EE = 0.43 V/nm).

Figure S6 – Orientation angles of three DEANST molecules without (on the left) and with (on the right, EE = 0.43 V/nm) electric field in the presence of THF only, and THF and MTE-1

Figure S7 – On the left: Orientation angles of three PN1 molecules with the electric field being 0.43 V/nm in the presence of THF only, and THF and MTE-1. On the right: Evolution of orientation angles in time for three individual PN1 molecules in THF and MTE-1.

Figure S8 – Orientation angles for molecules 2 – 5 without and with electric field. Electric field being 0.43 V/nm.

1. Summary

Influence of the viscosity of the solvent on the molecular motions, orientation of the molecule in the electric fields, the evaporation process, and concentration effects were successfully studied and described by molecular dynamic (MD) simulations. Our calculations have shown that the presence/absence of electric fields and the length of solvent molecules (degree of polymerization, viscosity) influence the motion of the molecules of interest. Moreover, by specific and targeted substitutions of donor and acceptor groups, we were able to design novel molecules suitable for optical power limiting (OPL) purposes. The successful results of our theoretical work have stimulated our experimental partners at the Swedish Defence Research Agency (Dr. Cesar Lopes) and University of Lyon (Prof. Stephane Parola) to develop synthetic protocols and equipment to produce ordered bulk glass materials in the laboratory. The status and description of this experimental work is left out from this report and we direct questions in this regard to Dr. Lopes (email: cesar.lopes@foi.se).

2. Introduction

High-power lasers can destroy optical sensors [1], and therefore the demand for sensor protection devices against powerful light has increased. Such protection can be achieved by OPL materials, which should have high transmission for low-intensity light and reduction in the transmitted power at higher intensities. Several materials have been studied within the context of OPL, among them the platinum(II) acetylides [2,3] being widely investigated for their photophysical and structural properties.

Here, we study movements and orientations of chromophores with a main objective being to produce glass materials for OPL purposes with ordered chromophores; this will be done by applying electric field to achieve passive sensor protection against laser damage. The theoretical study should reveal the interplay between the strength of the external field and the chromophore behavior in order to help prepare glass materials in the laboratory.

3. Methodology

Geometry (Fig. 1) optimizations, energy and the ESP charges calculations were carried out using density functional theory with the B3LYP exchange-correlation functional [4] and in combination of the 6-31G* basis set for DEANST and PFF; and the 6-31G* and 6-31G basis sets [5,6] for carbon and hydrogen, respectively, for PN1 and PE2. The Stuttgart (SDD) relativistic effective core potential was used for platinum and phosphorus atoms [7,8]. Calculations were performed with the Gaussian09 software package [9].

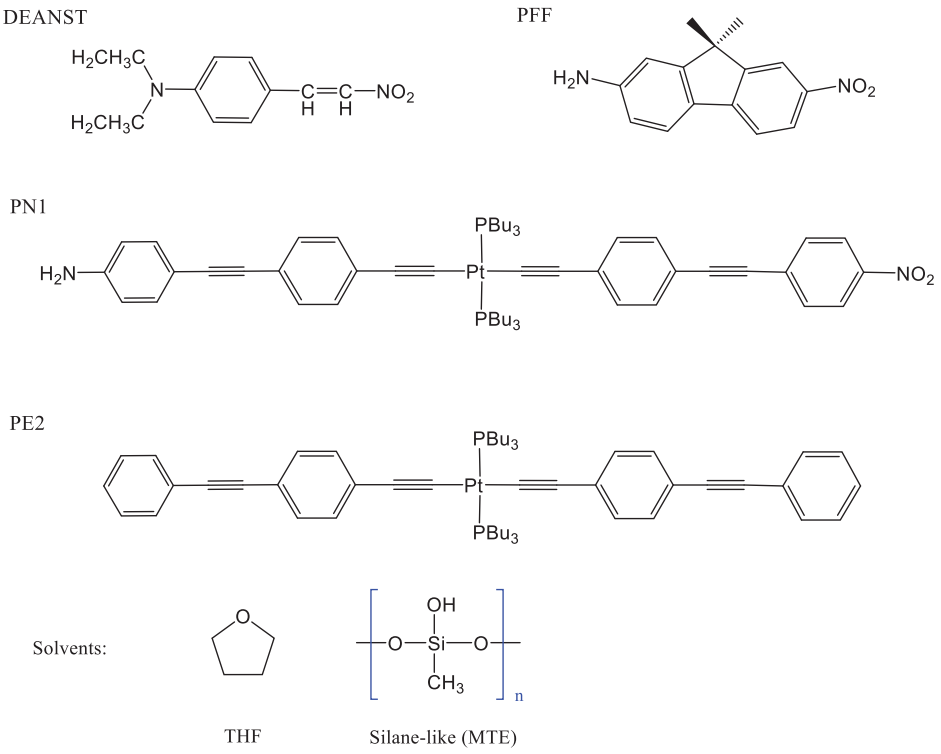

Figure 1: Molecular structures.

All MD simulations were carried out using the Amber 14 and/or Amber 16 packages [10, 11]. The initial boxes of solvent and chromophore molecules were prepared using the PACKMOL [12] package according to the following mixes:

a) THF + chromophore
b) THF (60 % weight) + MTE-1 (40 % weight) + chromophore
c) THF (60 %) + MTE-3 (40 %) + chromophore
d) THF (60 %) + MTE-5 (40 %) + chromophore
e) THF (60 %) + MTE-7 (40 %) + chromophore

where *n* in MTE-*n* stands for degree of polymerization.

Topologies and initial coordinates of each box were created using the LEaP program with the general Amber force field (GAFF) [13] that contains full sets of parameters for almost all the molecules of interest. Parameters for non-standard atoms not included in GAFF (platinum and silicon) were explicitly added based on Refs. [14-17]. The boxes were first created by PACKMOL and then equilibrated to reach a proper density. The MD simulations were performed at 300 K using Langevin dynamics and constant pressure periodic boundary with an average pressure of 1 atm and with isotropic position scaling using the

Berendsen barostat [18]. The simulations ran for 40 ns (if not stated otherwise) with a time step of 2 fs, the trajectories were recorded every 5,000 step and the cut-off were set to 12 Å for non-bonded interactions. All simulations were performed both with and without external static electric fields.

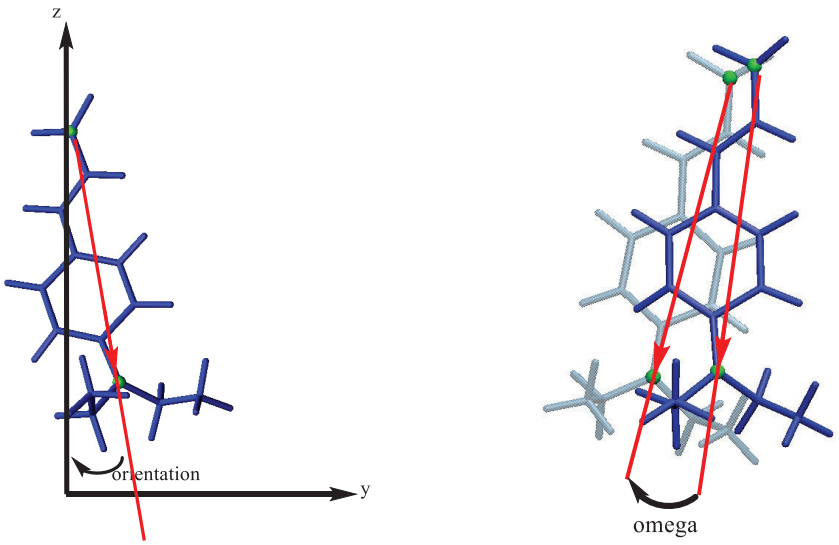

Figure 2: Orientation (left) and omega (right) angles. The angle omega, as defined in the text, represents the angle between two subsequent frames as illustrated in light and dark blue colors (nitrogen atoms are in green) and thus corresponds to an angular velocity.

4. Results and Discussion

4.1. Without externally applied electric fields

In the presence of THF only, DEANST does not have a preferential orientation and freely rotates in the box, as can be seen from the distribution (Fig. 3, left orientation panels) of the vector between the two nitrogen atoms (defined in Fig. 2). The angle omega (as illustrated in Fig. 2) is defined as the angle between the molecular orientations found in two subsequent frames separated by 10 ps and thus in reality it corresponds to an angular velocity. This angle is changing between 0 - 60° as seen in Fig. 3, right panels. The angular velocities are smaller when THF is mixed with MTE-1 and they get even smaller when mixed with MTE-3, MTE-5, or MTE-7 suggesting that the higher the degree of polymerization the more viscous the environment is and the slower the molecule is rotating. Moreover, DEANST dissolved in the mix of THF and MTE-3, MTE-5, or MTE-7 does not freely rotate with respect to the environment. Instead, it is seen that certain angles are preferred, showing that the degree of polymerization strongly influences the chromophore orientation.

A very similar behavior is observed for PFF (see Fig. S1). For the more extended PN1 chromophore, however, the angular velocity is already quite small in pure THF and it gets even smaller when introducing MTE-1 and higher degree of polymerized MTE (Fig. 4, left panels). The NO_2 and NH_2 groups in PN1 appear to be responsible for specific solvent interactions as the angular velocities are lower compared to the case of PE2.

At the beginning of each MD simulation, the THF and MTE-*n* solvent molecules were placed at random in the box (see Fig. 5a). After 40 ns, the MTE molecules are found to have aggregated (see Figs. 5b-e). This aggregation is of course to be expected as the segregation of THF and MTE occurs in order to create glass materials.

Our calculations have shown that the presence/absence of the glass precursor and also the oligomeric length of MTE influence the motion of chromophores.

4.2. With externally applied electric fields

In our studies of the effect of external electric fields, we applied a series of electric fields with different strengths (0.001, 0.01, 0.035, 0.065, 0.11, 0.22, 0.43, 0.65, 0.87, and 1.0 V/nm) along the *z*-axis. We first studied the effect of these static electric fields on DEANST in pure THF. At the lowest selection of electric field strengths, there are no significant effect on the chromophore orientation but from strengths of 0.1 V/m and upward there are apparent signs of chromophore orientation (see Fig. 6). Based on these simulations, we chose for our further studies a field strength of 0.43 V/nm. This corresponds roughly to a field strength that is some ten times larger than what is believed to be possible to reach in the laboratory setup. Aware of this the discrepancy, we use such a large field strength to overcome our computational limitations on the simulation time, *i.e.*, we get more distinct and clear results available within a shorter timeframe. DEANST always reorients in the way as shown in Fig. 7, meaning that the dipole moment vector is parallel to the electric field direction. Even if the initial orientation of DEANST is opposite and anti-parallel compared to the expected final orientation, it reorients itself after *ca* 1 ns and falls back into a parallel orientation.

After applying the electric field, DEANST orients in the direction of the electric field when surrounded by pure THF as well as in mixes of THF and MTE-1, MTE-3, MTE-5, and MTE-7 as seen in Fig. 8. The angular velocities are similar as seen in the absence of electric field, although the changes between MTE-1, MTE-3, and MTE-5 are less pronounced. PFF behaves similarly (see Fig. S2). There is a small population of orientation angles between 90° to 180° for PFF in a mix of THF and MTE-7, but this is only due to the fact that it took *ca* 10 ns for the chromophore to orient in such a viscous environment (see Fig. S3).

Compared to the smaller chromophores, PN1 rotates much slower in pure THF and even more slowly when introducing MTE-*n* compared to the previous chromophores (angular velocities are shown in Fig. S4). PN1 orients quite fast in pure THF, whereas *ca* 4 ns is needed for orientation in a mix of THF and MTE-1 (see Fig. 9). The initial orientation plays a crucial role in more viscous environments and, in a mix of THF and MTE-3, MTE-5, and MTE-7, PN1 does not orient with the electric field even after 100 ns (see Fig. 9).

With a vanishing dipole moment, PE2 does not respond much to the electric field. In pure THF, PE2 rotates freely within a time window of 70 ns (see Fig. S5, left top panel). Specific effects of the electric field are also not seen when introducing MTE-*n*. For MTE-7, we see that the chromophore remains oriented along the electric field, but this just an effect of viscosity and not electric-field orientation.

4.3. Evaporation process

THF molecules are evaporated during the glass preparation, therefore the evaporation effect was studied for DEANST in mixes of THF and MTE-*n* environments. Evaporation was done in the absence of the electric field under the same conditions as described above. The simulations ran for 100 ns and the rate of evaporation was one molecule of THF every 40 ps. For all systems, the density increased from 1.05 g/cm^3 at the beginning of simulations to 1.36 ± 0.02 g/cm^3 at the end of the evaporation process and the volume decreased about three times (see Fig. 11).

4.4. Chromophore concentration effects

To study the concentration effect of chromophores and their orientation in the electric field, we performed MD simulations of three chromophores in pure THF only and a mix of THF and MTE-1. In the cases of both DEANST and PN1, all three molecules orient along the electric field direction (see Figs. S6 and S7), although it is noted that, for PN1 in a mix of THF and MTE-1, the response time is slower. We do, however, not find that it would be prohibitively hard to prepare glass materials with high concentrations of oriented chromophores as due to unfavorable dipole–dipole interactions.

4.5. Proposals of new OPL chromophores

In the design novel chromophores, we suggested five structures having two donor and two acceptor groups (see Fig. 12). The underlying reason for this molecular design strategy has to do with the geometry and design of the experimental setup of equipment for the glass preparation under strong electric fields. The external static electric field is applied during the phase of glass preparation in a direction parallel to the optical axis. As our chromophores are largely one-dimensional in their absorbing electromagnetic radiation

and energy, it becomes important to reach a chromophore orientation that is perpendicular to the optical axis.

Our simulations on this set of novel compounds show that, with an electric field strength of 0.43 V/nm, the long axis of molecule **1** orients in the desired direction (see Fig. 13). It orients even better when applying slightly higher field of 0.65 V/nm. In order to keep consistency with the previous results, the electric field was kept at 0.43 V/nm for molecules **2** – **5**, for which similar behavior is seen as the orientation angles are around 90° (see Fig. S8). All histograms are plotted for the vector shown in red color in Fig. 12 with respect to the *z*-axis, and all simulations were done in pure THF.

5. Conclusions

By means of molecular dynamic simulations in the absence or presence of electric fields, we studied the movement and orientation of molecular absorbers suitable for OPL applications. Based on our observations, we obtained smaller angular velocities for molecular rotations with increasing solvent polymerization suggesting, quite expectedly, that the more viscous the environment the slower the motion. The consequence of these findings for the experimental glass production is that the orientation must be achieved before significant oligomerization of the glass precursor takes place. Furthermore, we observed that quite high fields were required to orient the chromophore, at least on the short timescales of the simulations. The applied field strengths in the simulations are larger than what the planned experimental setup will allow for but, on the other hand, timescales in the real world are longer so it is deemed realistic to achieve an orientational effect in the laboratory. We have also designed several new compounds to fit the setup of experimental equipment in the process of glass production. We made use of two donor and two acceptor groups to reach an orientation of platinum(II) acetylide compounds where the conjugation axis is perpendicular to the optical axis.

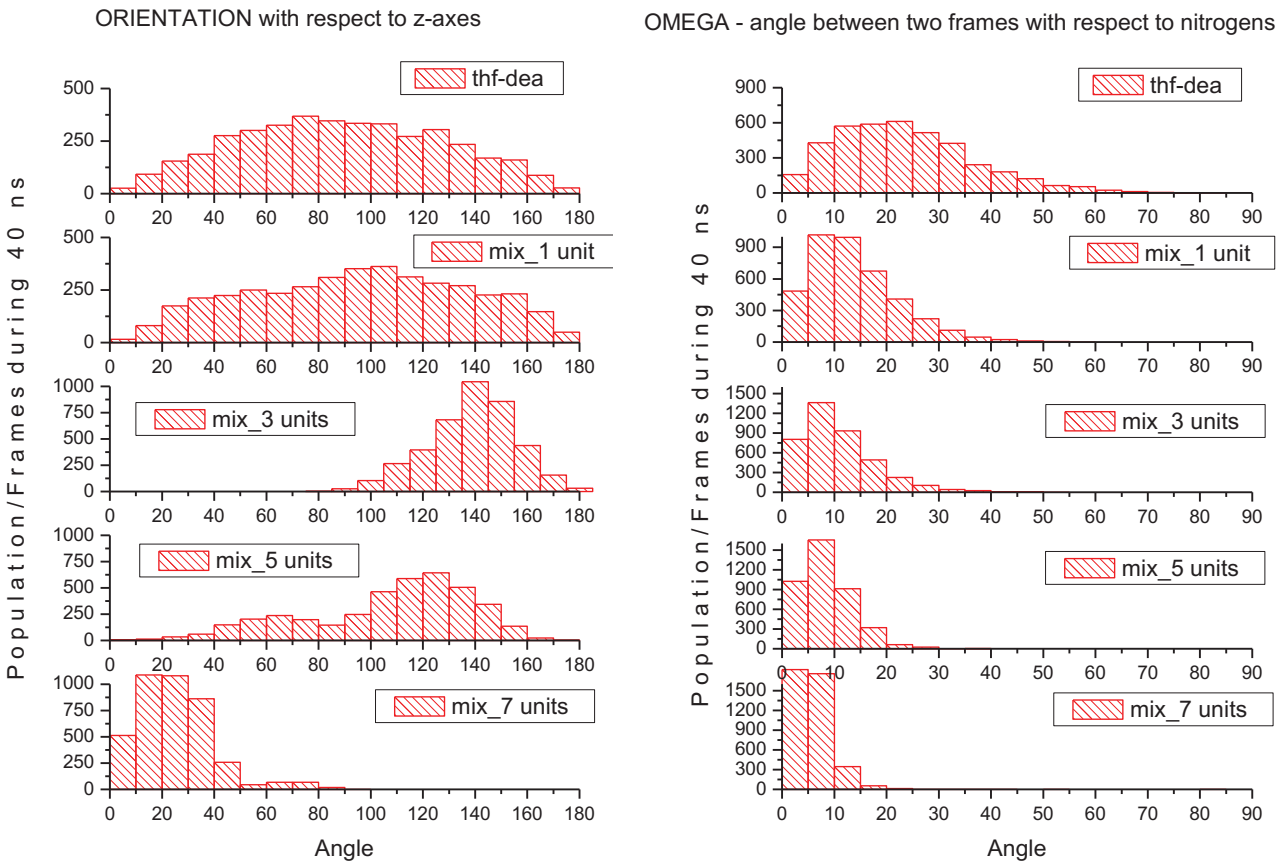

Figure 3: Angle populations for DEANST in the absence of electric fields.

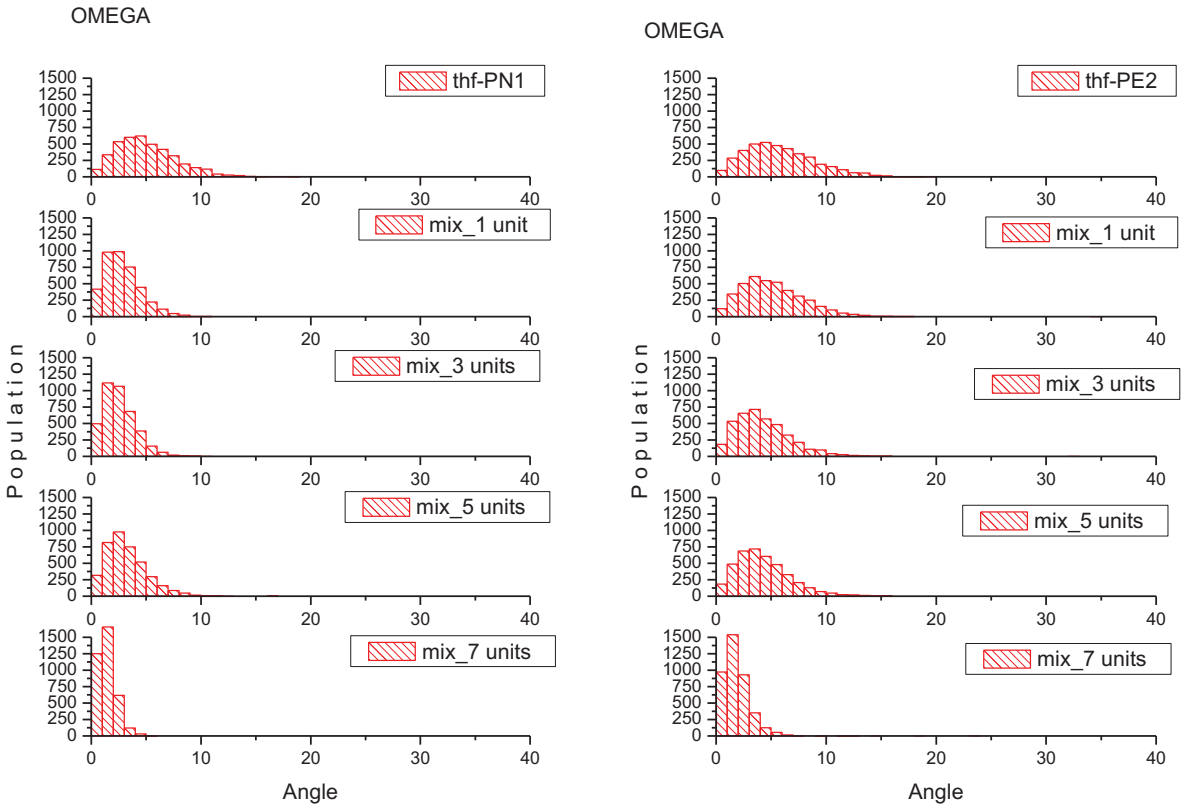

Figure 4: Angular velocities for PN1 (left) and PE2 (right) in the absence of electric fields.

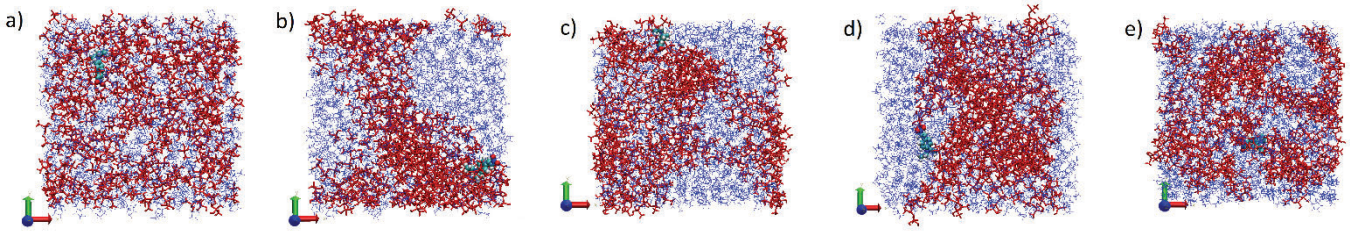

Figure 5: Initial (a) and final (b-e) simulation boxes of DEANST with THF and MTE-1 (b), MTE-3 (c), MTE-5 (d) and MTE-7 (e); THF is shown in blue and MTEs in red.

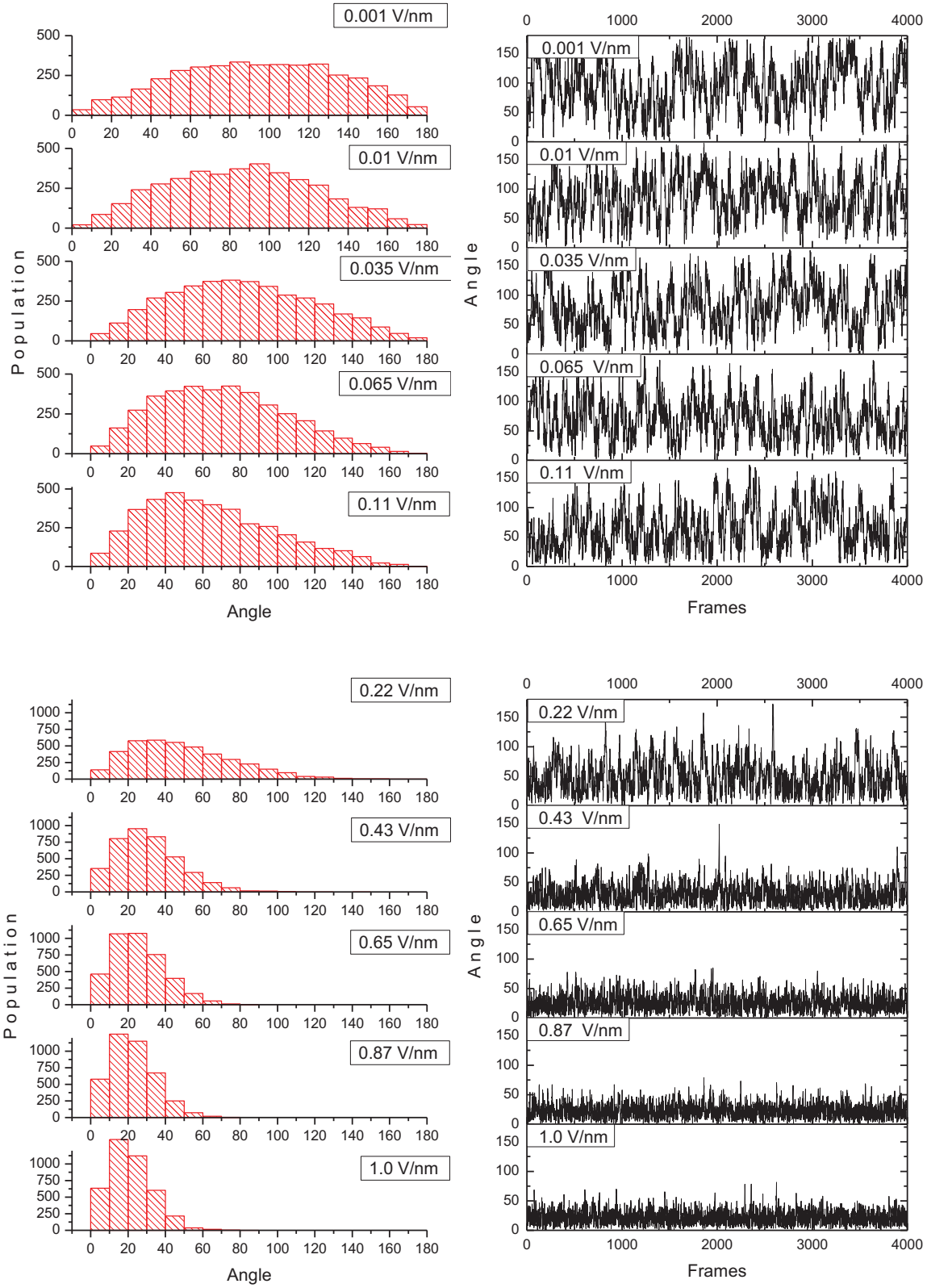

Figure 6: Population of the angles (left) for series of electric fields with different strength and their developments over time (right) for the DEANST molecule.

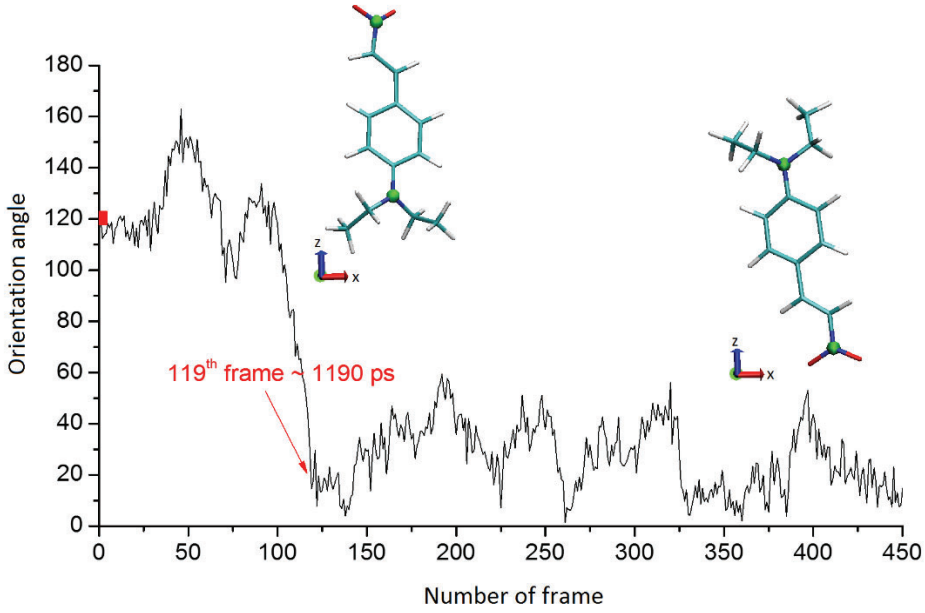

Figure 7: Beginning of MD simulation. DEANST in THF quickly orients in electric field (0.43 V/nm) from orientation on the left side (the $NO_2 \rightarrow NH_2$ vector being antiparallel to the electric field propagation) to the orientation on the right side (the $NO_2 \rightarrow NH_2$ vector being parallel to the electric field propagation).

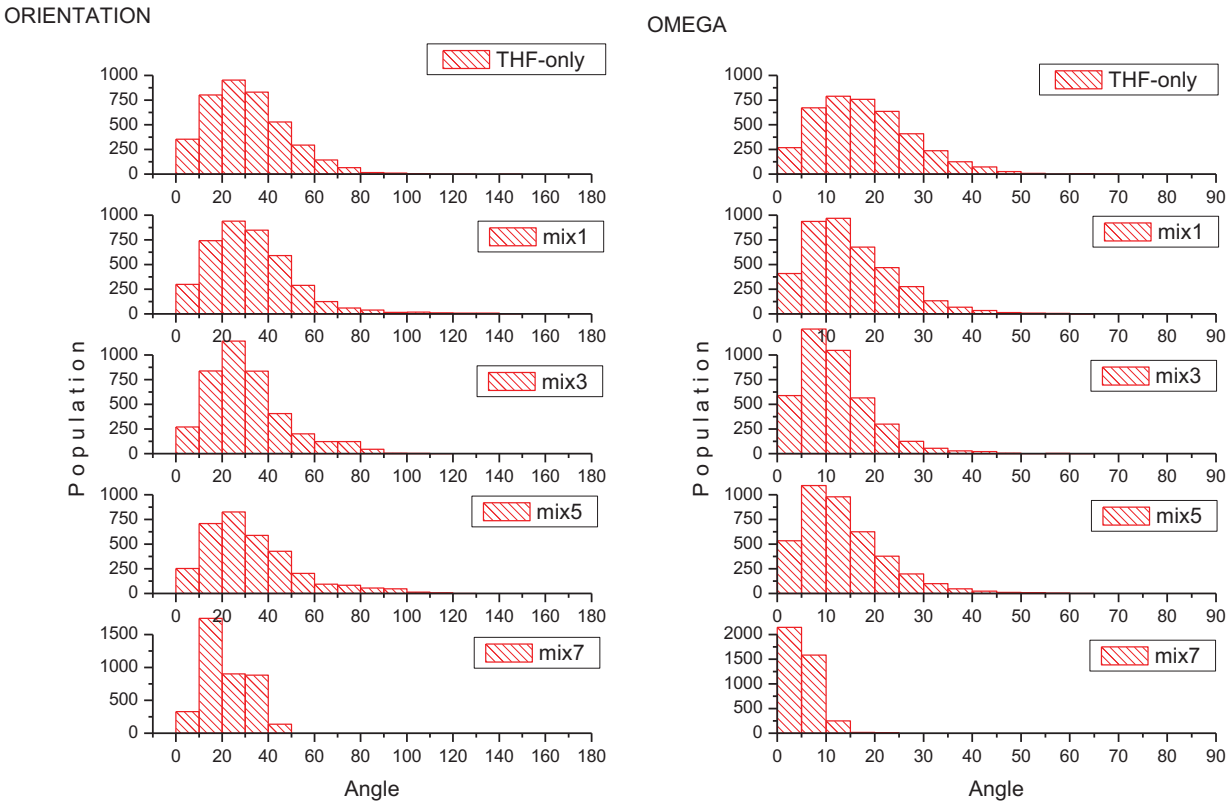

Figure 8: Population of the angles for DEANST in the presence of an electric field (0.43 V/nm).

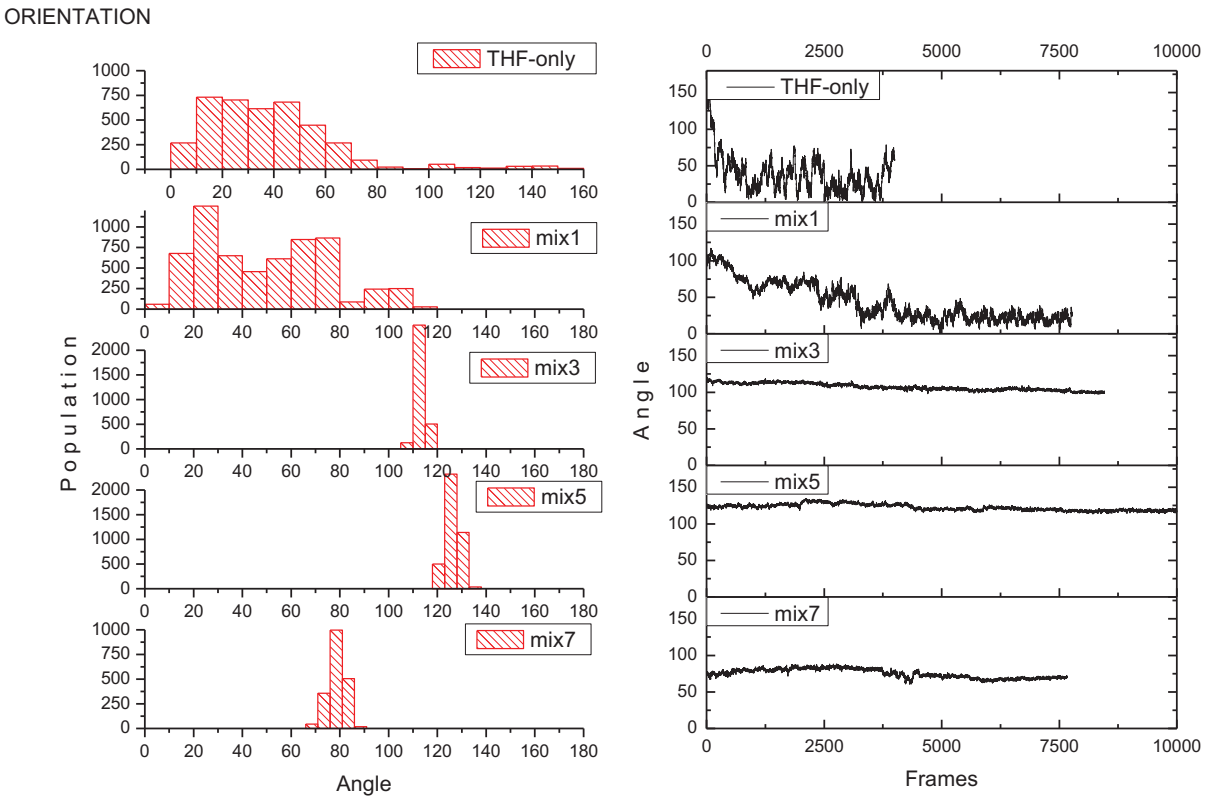

Figure 9: Population of PN1 and its development over time in the presence of electric field (0.43 V/nm).

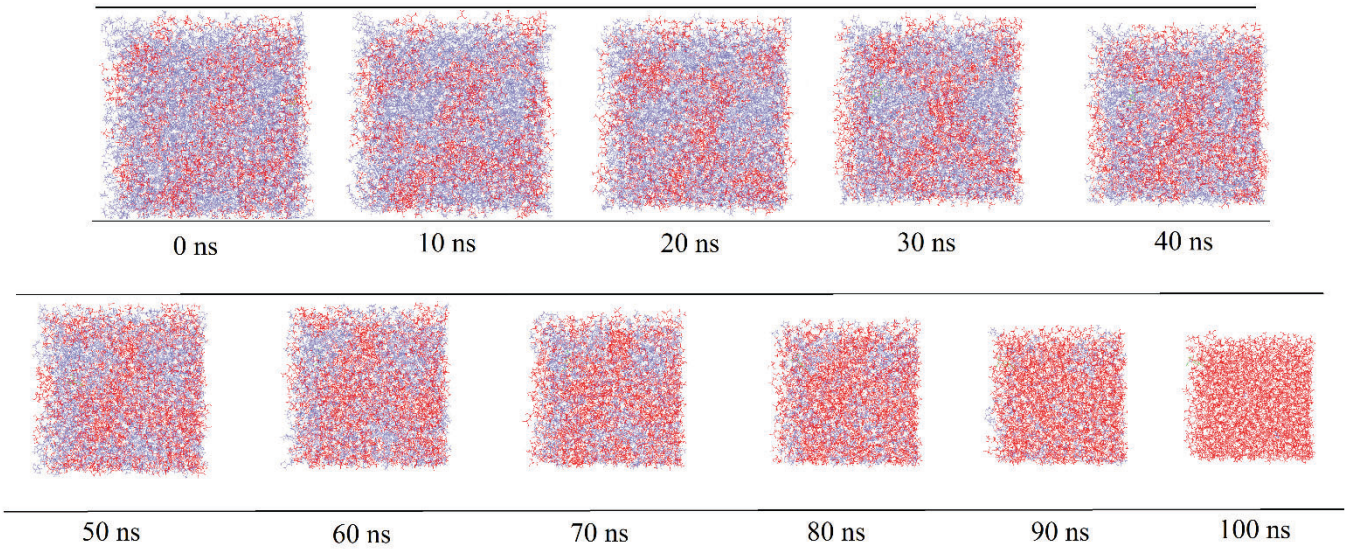

Figure 10: Evolution of evaporation process for DEANST. MTE-1 is shown in red, THF in blue.

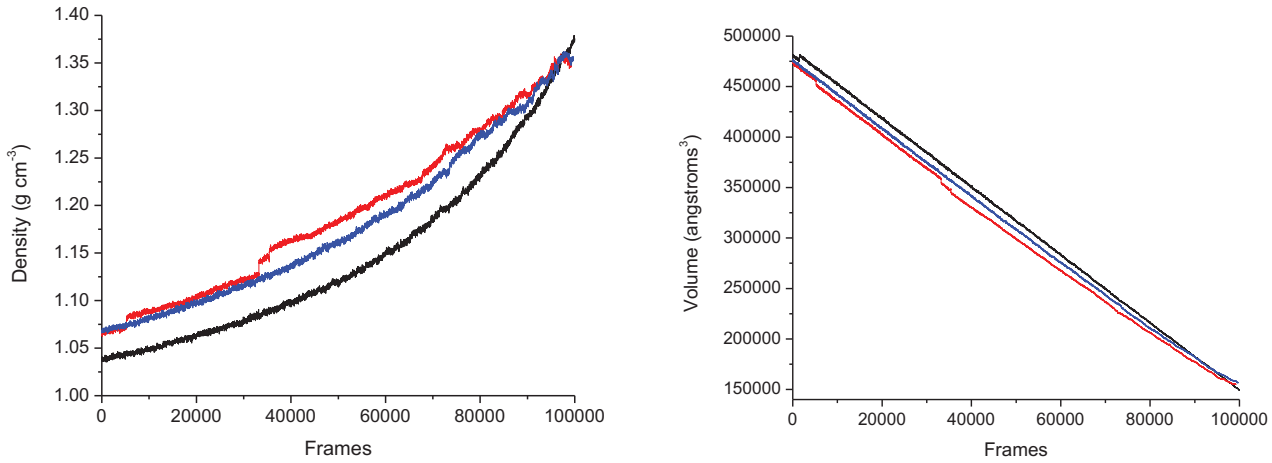

Figure 11: Density (left) and volume (right) evolvements during the evaporation effect. Black curve corresponds to the box with THF and MTE-1, the red curve to THF and MTE-3, and the blue curve to THF and MTE-5.

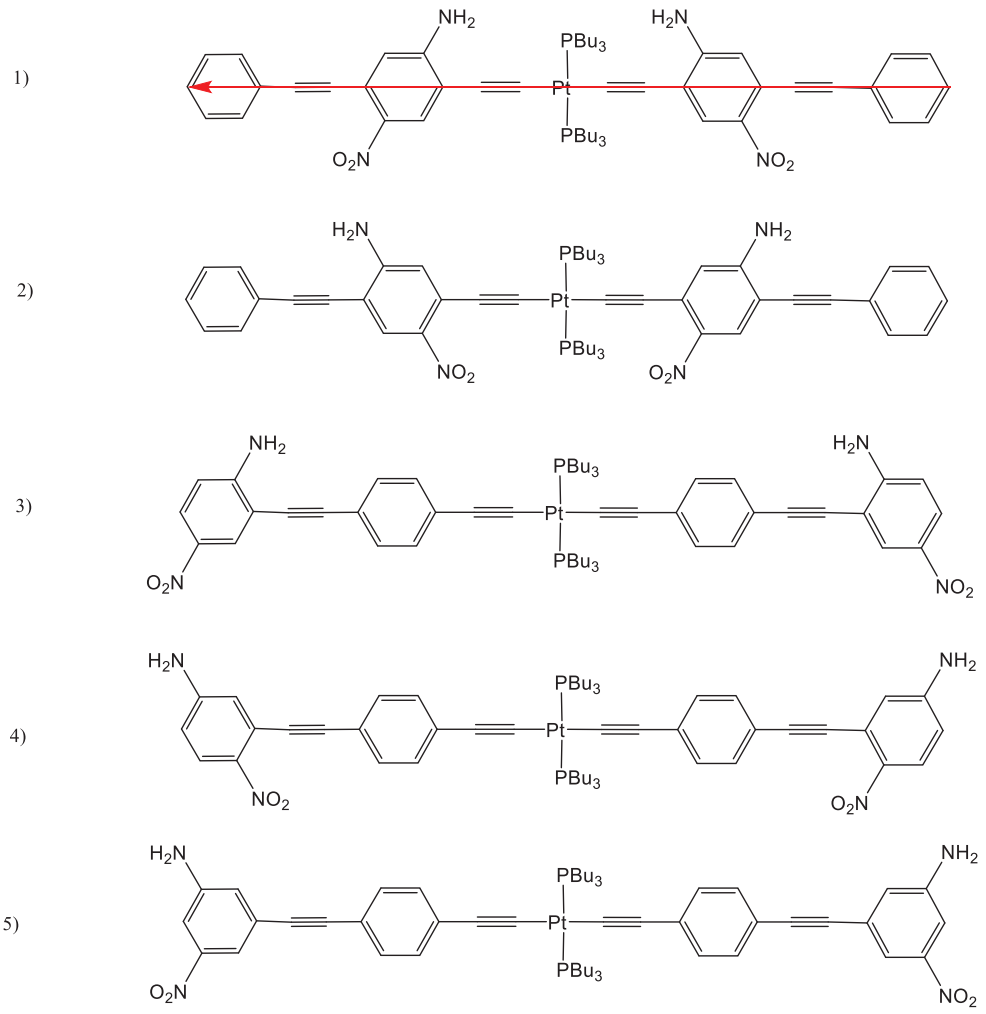

Figure 12: Proposed structures of of novel chromophores. The red vector shows the conjugation axis of the system, also used to evaluate the orientation angle with respect to the external electric field.

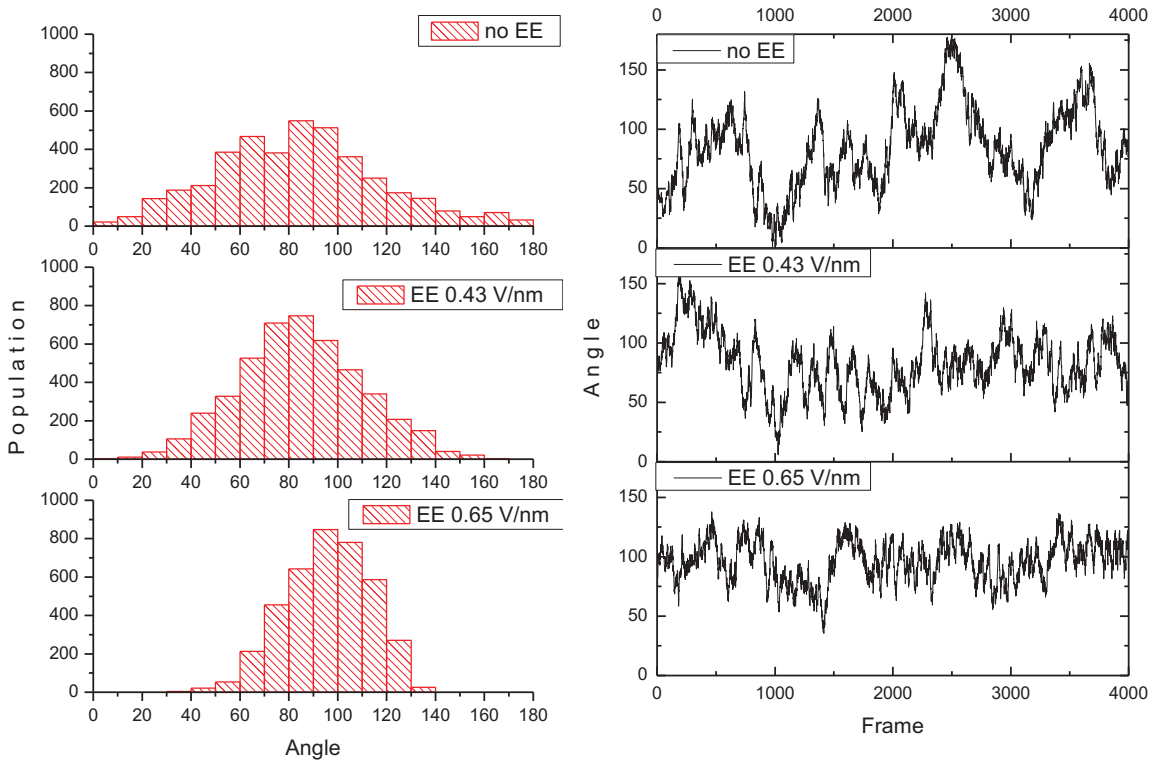

Figure 13: Populations of the orientation angles for molecule **1** in Fig. 12 and their developments over time.

6. References

[1] Ch. W. Spangler: Recent development in the design of organic materials for optical power limiting. Journal of Materials Chemistry 9, 2013-2020 (1999)

[2] E. Glimsdal, P. Norman, M. Lindgren: Excitation and Emission Properties of Platinum(II) Acetylides at High and Low Concentrations. Journal of Physical Chemistry A 113, 11242-11249 (2009)

[3] T. M. Cooper, J. E. Haley, D. M. Krein, A. R. Burke, J. E. Slagle, A. Mikhailov, A. Rebane: Two-Photon Spectroscopy of a Series of Platinum Acetylides: Conformation-Induced Ground-State Symmetry Breaking. Journal of Physical Chemistry A 121, 5442-5449 (2017)

[4] A. D. Becke: Density functional thermochemistry. III. The role of exact exchange. The Journal of Chemical Physics 98, 5648-5652 (1993)

[5] W. J. Hehre, R. Ditchfield, and J. A. Pople: Self-Consistent Molecular Orbital Methods. XII. Further Extensions of Gaussian—Type Basis Sets for Use in Molecular Orbital Studies of Organic Molecules. The Journal of Chemical Physics 56, 2257-2261 (1972)

[6] P. C. Hariharan and J. A. Pople: The Influence of Polarization Functions on Molecular Orbital Hydrogenation Energies. Theoret. Chim. Acta 28, 213--222 (1973)

[7] A. Bergner, M. Dolg , W. Küchle , H. Stoll, H. Preuss: Ab initio energy-adjusted pseudopotentials for elements of groups 13–17. Molecular Physics 80, 1431-1441 (1993)

[8] D. Andrae, U. Häussermann, M. Dolg, H. Stoll, H. Preuss: Energy-adjusted ab initio pseudopotentials for the second and third row transition elements. Theoret. Chim. Acta 77, 123-141 (1990)

[9] Gaussian 09, Revision D.01, M. J. Frisch, G. W. Trucks, H. B. Schlegel, G. E. Scuseria, M. A. Robb, J. R. Cheeseman et al., Gaussian, Inc., Wallingford CT, 2013.

[10] D.A. Case, V. Babin, J.T. Berryman, R.M. Betz, Q. Cai, D.S. Cerutti, T.E. Cheatham, III, T.A. Darden, R.E. Duke, H. Gohlke, A.W. Goetz, S. Gusarov, N. Homeyer, P. Janowski, J. Kaus, I. Kolossváry, A. Kovalenko, T.S. Lee, S. LeGrand, T. Luchko, R. Luo, B. Madej, K.M. Merz, F. Paesani, D.R. Roe, A. Roitberg, C. Sagui, R. Salomon-Ferrer, G. Seabra, C.L. Simmerling, W. Smith, J. Swails, R.C. Walker, J. Wang, R.M. Wolf, X. Wu and P.A. Kollman (2014), AMBER 14, University of California, San Francisco.

[11] D.A. Case, R.M. Betz, D.S. Cerutti, T.E. Cheatham, III, T.A. Darden, R.E. Duke, T.J. Giese, H. Gohlke, A.W. Goetz, N. Homeyer, S. Izadi, P. Janowski, J. Kaus, A. Kovalenko, T.S. Lee, S. LeGrand, P. Li, C. Lin, T. Luchko, R. Luo, B. Madej, D. Mermelstein, K.M. Merz, G. Monard, H. Nguyen, H.T. Nguyen, I. Omelyan, A. Onufriev, D.R. Roe, A. Roitberg, C. Sagui, C.L. Simmerling, W.M. Botello-Smith, J. Swails, R.C. Walker, J. Wang, R.M. Wolf, X. Wu, L. Xiao and P.A. Kollman (2016), AMBER 2016, University of California, San Francisco.

[12] L. Martínez, R. Andrade, E. G. Birgin, J. M. Martínez. Packmol: A package for building initial configurations for molecular dynamics simulations. Journal of Computational Chemistry 30, 2157-2164, 2009.

[13] J. Wang, R. M. Wolf, J. W. Caldwell, P. A. Kollman, D. A. Case: Development and Testing of a General Amber Force Field. Journal of Computational Chemistry 25, 1157-1174, 2004

[14] D.A. Case, D.A. Pearlman, J.W. Caldwell, T.E. Cheatham III, J. Wang, W.S. Ross, C.L. Simmerling, T.A. Darden, K.M. Merz, R.V. Stanton, A.L. Cheng, J.J. Vincent, M. Crowley, V. Tsui, H. Gohlke, R.J. Radmer, Y. Duan, J. Pitera, I. Massova, G.L. Seibel, U.C. Singh, P.K. Weiner and P.A. Kollman (2002), AMBER 7 (Appendix C: Parameter Development), University of California, San Francisco.

[15] J. Sjoqvist, M. Linares, P. Norman: Platinum (II) and phosphorus MM3 force field parametrization for chromophore absorption spectra at room temperature. The Journal of Physical Chemistry A 114, 4981-4987, 2010.

[16] J. M. Shorb, B. P. Krueger, M. E. Silver: Development of Parameters for Modeling Silicon-Oxygen Polymers in AMBER Molecular Dynamics Simulations. Hope College, Holland, MI 49423, http://www.chem.hope.edu/~krieg/shorb/ (March, 2003)

[17] H. Sun, D. Rigby: Polysiloxanes: ab initio force field and structural, conformational and thermophysical properties. Spectrochimica Acta Part A 53, 1301-1323, 1997

[18] H. J. C. Berendsen, J. P. M. Postma, W. F. van Gunsteren, A. DiNola, and J. R. Haak: Molecular dynamics with coupling to an external bath. J. Chem. Phys. 81, 3684-3690, 1984.

7. List of Abbreviations

MD	molecular dynamic	GAFF	general Amber force field
OPL	optical power limiting	EE	electric field
THF	tetrahydrofuran	MTE	silane-like glass precursor solvent

8. Supplementary information

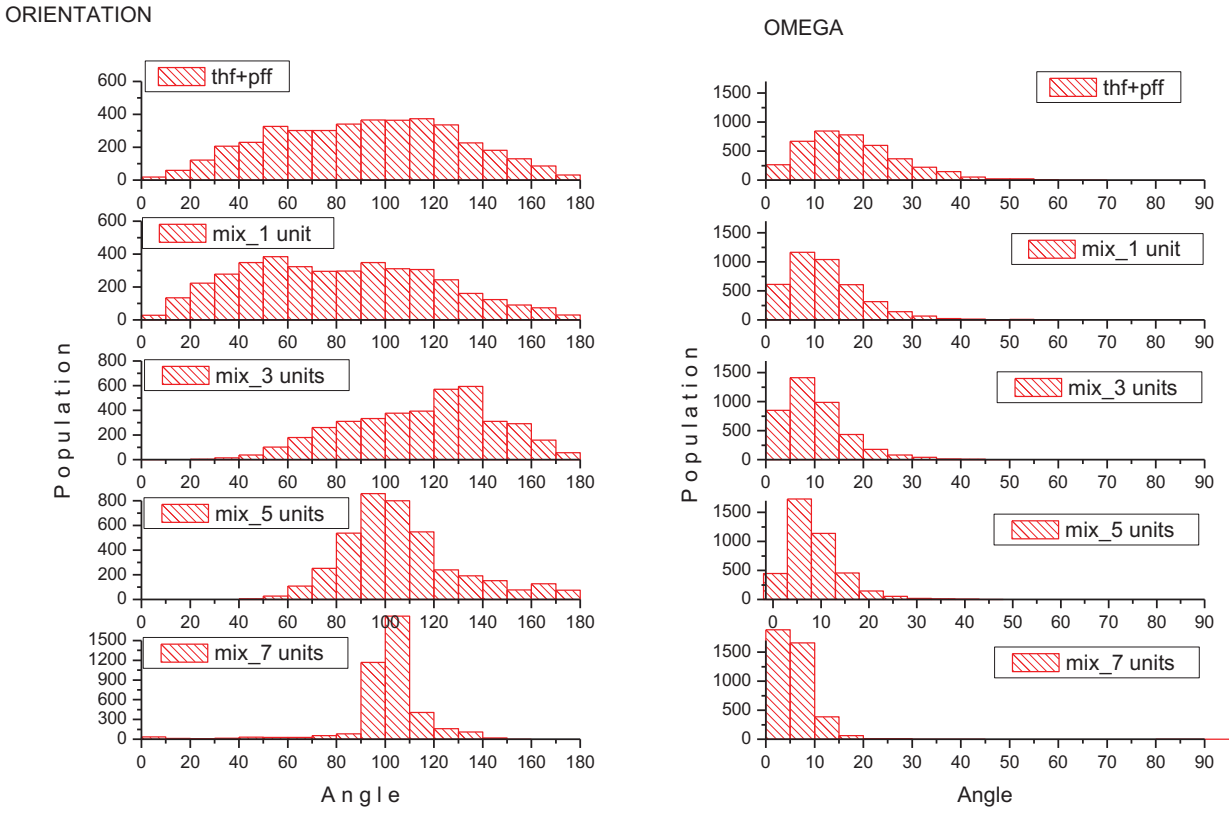

Figure S1 – Orientation and omega angles' population of PFF in the absence of electric field.

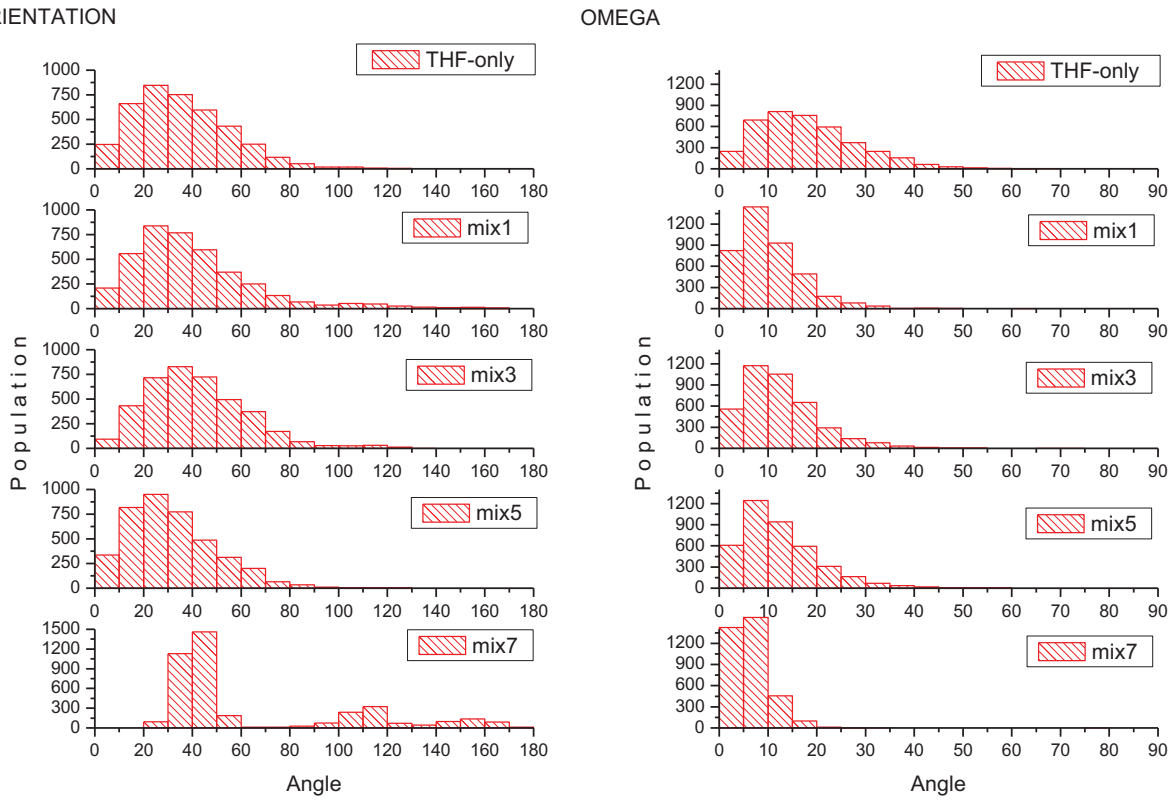

Figure S2 – Orientation and omega angles' population of PFF in the presence of electric field (EE = 0.43 V/nm). Detailed time development for PFF in THF and MTE-7 shown in Fig. S3.

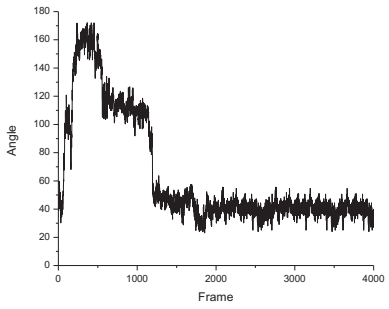

Figure S3 – PFF in THF and MTE-7 and its development over a period of 40 ns.

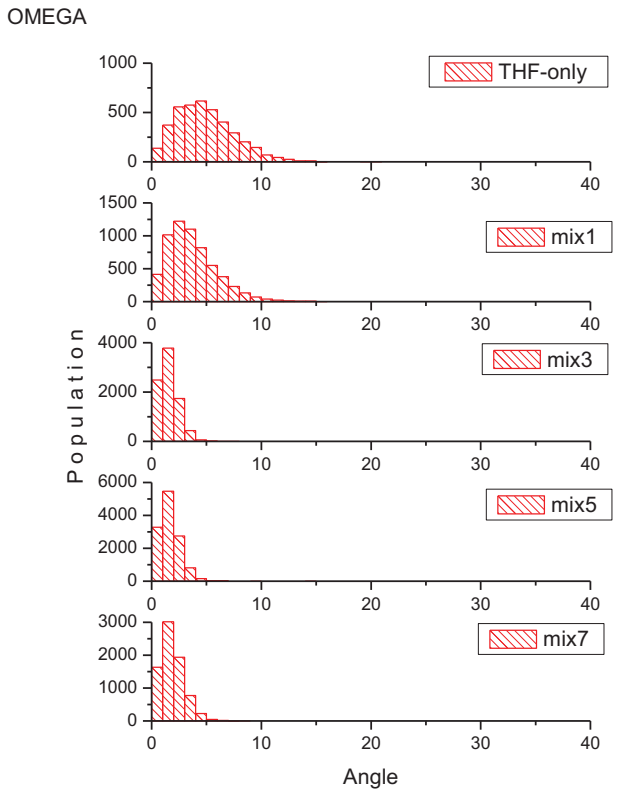

Figure S4 – Omega angles' population for PN1 with the electric field (EE = 0.43 V/nm).

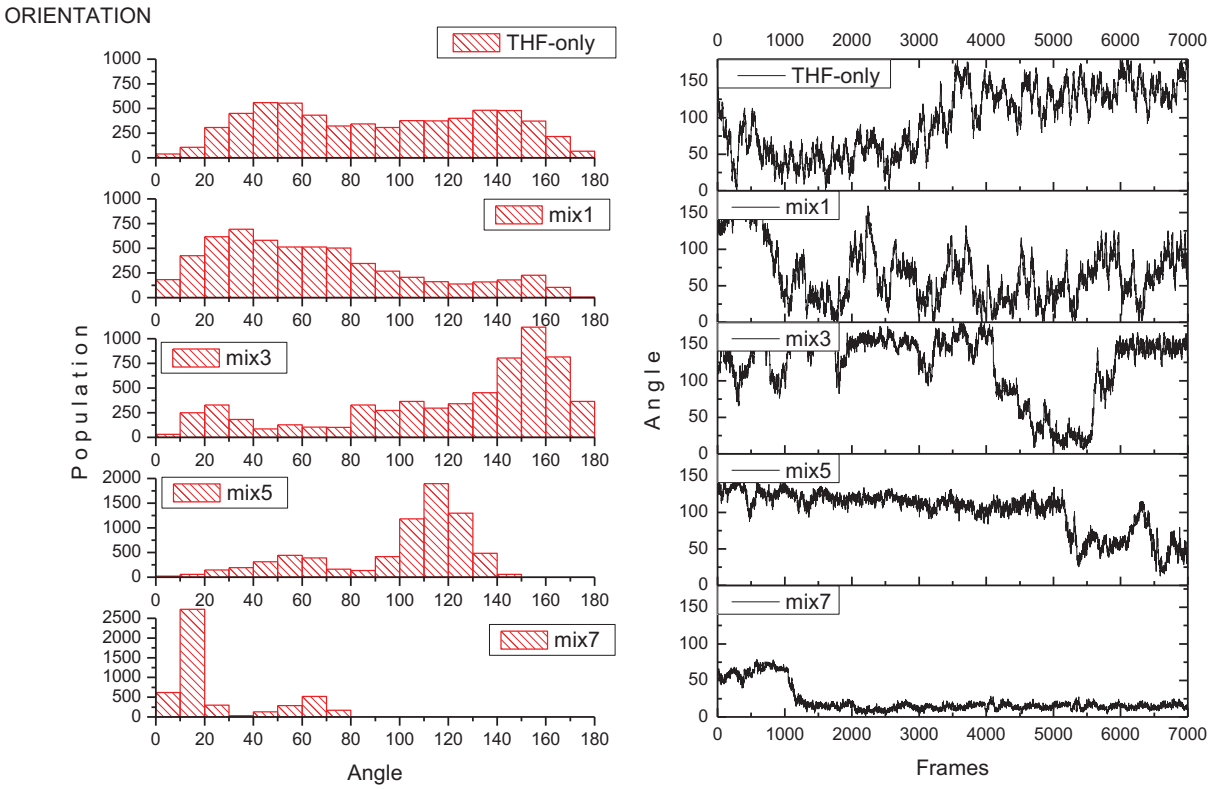

Figure S5 – Population of PE2 and its development over time in electric field (EE = 0.43 V/nm).

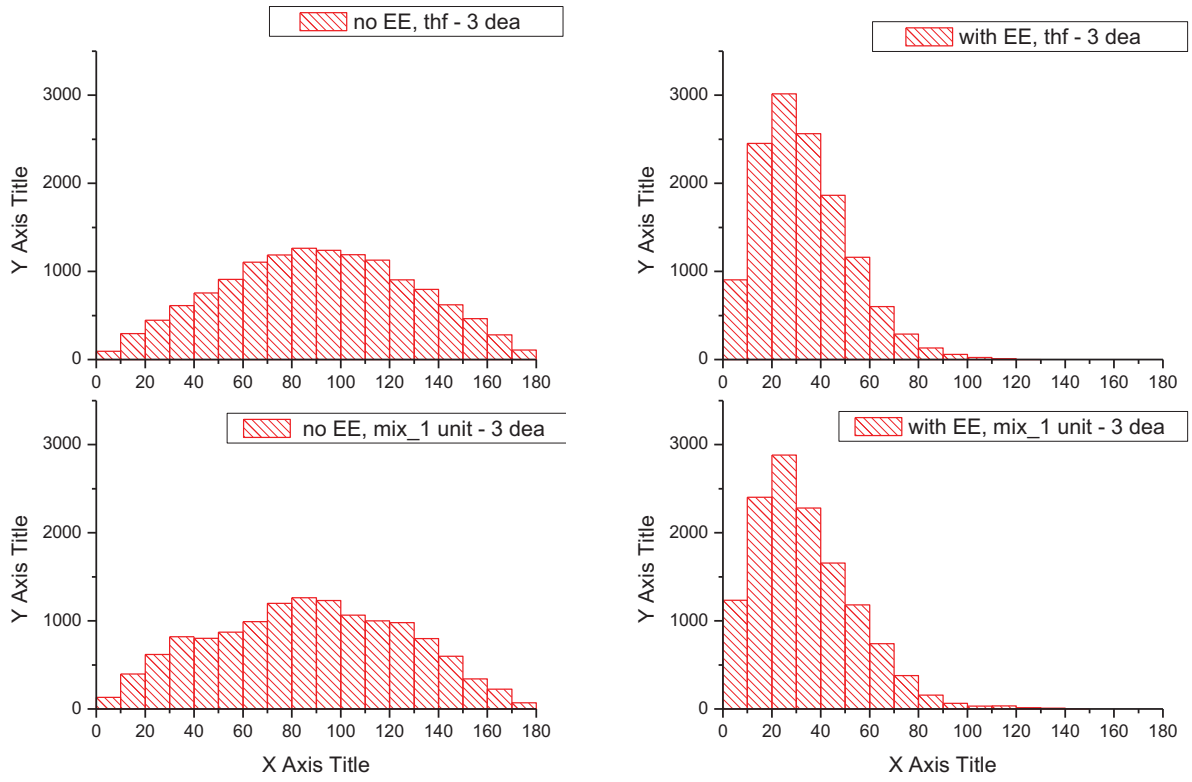

Figure S6 – Orientation angles of three DEANST molecules without (on the left) and with (on the right, EE = 0.43 V/nm) electric field in the presence of THF only, and THF and MTE-1

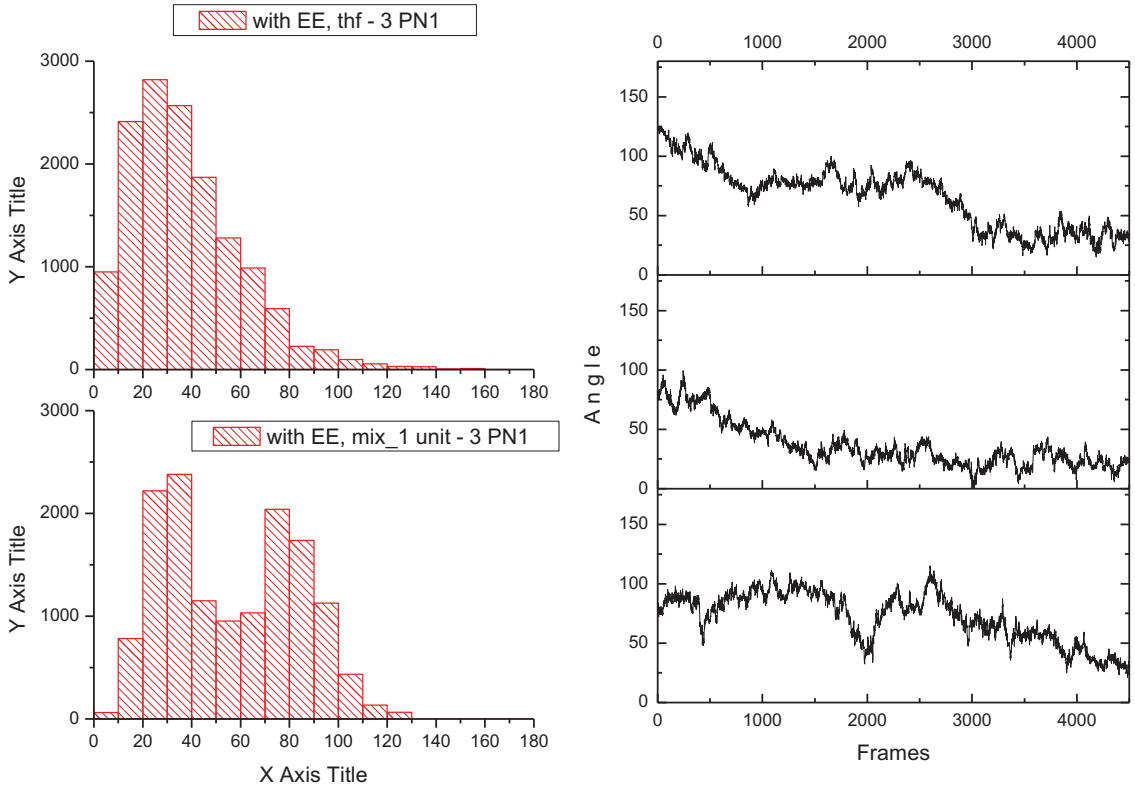

Figure S7 – On the left: Orientation angles of three PN1 molecules with the electric field being 0.43 V/nm in the presence of THF only, and THF and MTE-1. On the right: Evolution of orientation angles in time for three individual PN1 molecules in THF and MTE-1.

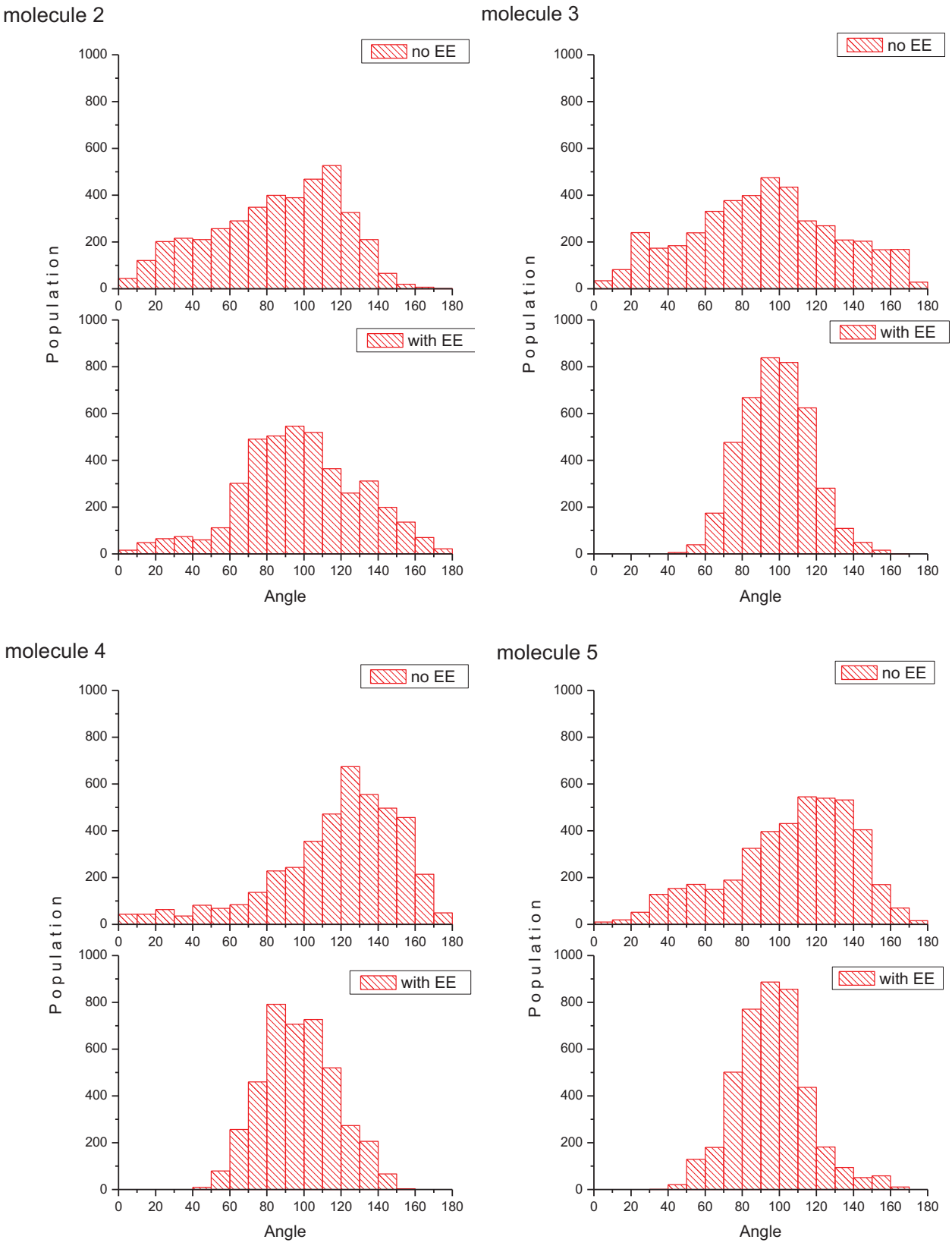

Figure S8 – Orientation angles for molecules **2** – **5** without and with electric field. Electric field being 0.43 V/nm.